Journal of Environmental Chemical Engineering 10 (2022) 108012

Contents lists available at ScienceDirect

Journal of Environmental Chemical Engineering

journal homepage: www.elsevier.com/locate/jece

Influence of interaction on accuracy of quantification of mixed microplastics using Py-GC/MS

Fangfang Lou, Jun Wang, Chen Sun, Jiaxing Song, Wanli Wang, Yuhan Pan, Qunxing Huang *, Jianhua Yan

State Key Laboratory of Clean Energy Utilization, Institute for Thermal Power Engineering, Zhejiang University, Hangzhou 310027, China

ARTICLE INFO

Editor: Teik Thye Lim

Keywords:
Microplastics
Quantification
Co-pyrolysis
Interaction
Py-GC/MS

ABSTRACT

Accurate identification and quantification are very challenging and extremely important in evaluating microplastic (MP) pollution. Although pyrolysis-based MP measurement methods have attracted intensive interest due to their great potential for rapid qualitative and quantitative analysis, the influence of thermochemical interactions during co-pyrolysis of different plastics has not been addressed. In the present study, five common MP materials, polyethylene (PE), polypropylene (PP), polystyrene (PS), polyvinyl chloride (PVC), and polymethyl methacrylate (PMMA), were detected using pyrolysis gas chromatography mass spectrometry (Py-GC/MS). The existence of interactions was confirmed by comparing the experimental results of individual and mixed pyrolysis. Upon the specific analysis of the impact on the quantitative calculation, we found that some indicators selected in previous studies may lead to high uncertainty, exceeding 100%. On this basis, new indicators with better reliability were proposed for the quantitative analysis of mixed MP samples, including 1- octadecene, pentane, and bibenzyl. Finally, the maximum quantification uncertainties of PE, PP, and PS were reduced from 91–25%, 130–32%, and 93–24%, respectively. The present study can provide a reference for improving the accuracy of quantitative analysis of mixed MPs.

1. Introduction

Microplastics (MPs) are one type of plastic pollution in the environment, but are smaller in size than conventional plastic waste. In 2004, Thompson et al. [1] put forward the concept of MPs. In 2009, the National Oceanic and Atmospheric Administration (NOAA) defined the upper size limit of MPs as 5 mm [2]. Primary MPs that are mainly used for personal care products are produced in this size (<5 mm). While secondary MPs are results of bigger plastic products fragmentation.

The confusing appearance of MPs makes them easy to be ingested by lower organisms, thus endangering their health [3–7]. Accumulated MPs in organisms could cause internal abrasions and blockages [8,9]. In addition, plastic additives and attached contaminants, such as heavy metals [10,11] and organic pollutants [12–14] may cause cancer and endocrine disruption. These hazards can be bioaccumulated and biomagnified through the food chain, and thus endanger human health [15]. MPs are currently one of the emerging pollutants.

The composition and concentration of MPs are of great significance in assessing the level of environmental pollution and investigating the toxic effects of MPs. However, a standard evaluation system for MP pollution has not been established up to date.

In the early years, the identification and enumeration of MPs were mainly based on visual observation [16,17], which can result in the misjudgment of ~32% of plastic particles and ~25% of plastic fibers [18]. This is due to: (1) the difficulty in distinguishing natural fibers from artificial fibers by morphological features, (2) the tendency to miss colorless plastic particles, and (3) the interference of contaminants in the environment [19,20].

At present, the mainstream methods for microplastics detection include vibrational spectroscopy and pyrolysis, which respectively correspond to particle number concentration detection and mass concentration detection. The most common particle number concentration detection is through the combination of vibrational spectroscopy (represented by Fourier transform infrared spectroscopy [21,22] and Raman spectroscopy [21–24]) and imaging techniques, which allows for particle counting while detecting MPs components. However, the original MPs may continue to age and disintegrate into smaller fragments [25], even in the detection process, resulting in the change of number

* Corresponding author.
E-mail address: hqx@zju.edu.cn (Q. Huang).

https://doi.org/10.1016/j.jece.2022.108012
Received 28 February 2022; Received in revised form 27 May 2022; Accepted 29 May 2022
Available online 1 June 2022
2213-3437/© 2022 Elsevier Ltd. All rights reserved.

concentration. In addition, the number concentrations obtained from different studies are inappropriate for comparison since the minimum and maximum sizes considered by studies may be inconsistent. For example, both Imhof et al. [26] and Mani et al. [27] studied the content of MPs in sediments. However, the lower size limits in the two studies were 1 μm and 10 μm, respectively, due to differences in detection methods. In summary, the characterization of MP content in samples using particle number concentrations could not sufficiently accurate in some cases.

Comparatively, the mass concentration reflects the contamination level of MPs more accurately and uniformly. Although the application of thermal methods in MPs detection is still in the initial stage, it is very suitable for the mass concentration detection. Ribeiro et al. [28] used pyrolysis gas chromatography mass spectrometry (Py-GC/MS) to detect the MP content in five types of Australian seafood. Liu et al. [29] explored the application of thermogravimetric analysis-Fourier transform infrared-gas chromatography-mass spectrometry (TGA-FTIR-GC/MS) to identify MPs in mussel samples from China. Goedecke et al. [30] compared the suitability of four thermal analysis methods for MPs, including thermal extraction desorption-gas chromatography/-mass spectrometry (TED-GC/MS), TGA-FTIR, TGA-MS, and microscale combustion calorimeter (MCC). Through combination spectroscopy, chromatography, and mass spectrometry, thermal analysis allows the simultaneous detection of MP composition and content. This has become a future trend in quantitative detection [31–34].

In the application of thermal analysis, interactions between different components may occur. With the current extraction technologies, MPs isolated from environmental samples (e.g., water, sediment, animal tissue) are often mixed. Ribeiro et al. [28] quantified four kinds of polymers, polyethylene (PE), polypropylene (PP), polystyrene (PS), and polyvinyl chloride (PVC), from a *Portunus armatus* tissue sample. In the research by Kirstein et al. [35] on MP pollution of drinking water, most of the extracted samples were mixtures of multiple plastics (2–6 kinds), including PE, PS, polyurethane (PU), PP, polyamide (PA), and PVC. Co-pyrolysis inevitably occurs during the testing of mixed MP samples [34,36]. Although previous studies have pointed out interactions in polymer co-pyrolysis [37–41], few existing MPs studies have investigated this phenomenon, especially its impact on quantitative results.

The present study explored the influence of co-pyrolysis interaction on quantitative accuracy in the detection process. Five common MP materials, PE, PP, PS, PVC, and PMMA were chosen and their analytical pure samples were detected using Py-GC/MS. Under the same conditions, pyrolysis experiments of single and mixed components were carried out respectively. We confirmed the existence of the co-pyrolysis interaction through the comparison of products distribution and evaluated its influence on MPs quantitative detection. Finally, we chose new quantitative indicators to reduce the impact of interaction. Compared with previous MPs studies, the method and novel indicators proposed in this work can remarkably reduce calculation uncertainty and improve quantitative accuracy.

2. Materials and methods

2.1. Standard plastics materials

In the present study, five types of plastic samples commonly found in previous MP studies and currently in high yield were selected, including PE, PP, PS, PVC, and PMMA. These five kinds of polymer materials with analytical grade were purchased from Shanghai Yangli Electromechanical Technology Co., Ltd. The specific information of the reagents is shown in Table S1.

2.2. Py-GC/MS analysis

The pyrolysis system (Frontier Rx-3050TR) and GCMS (Shimadzu QP2010 Ultra) equipped with a low-polarity column (SH-Rxi-5Sil-MS) were used in the present study.

Rx-3050TR pyrolyzer is designed with two reactors, as shown in Fig. S1. The 1st reactor is a pyrolysis furnace, whose temperature was set at 650 °C, according to Ribeiro et al. [28]. While the 2nd section only serves as heat preservation (350 °C). We didn't set a higher temperature in the second reactor to avoid providing conditions for the second reaction. In addition, the residence time of pyrolysis gas in the tandem reaction chamber was calculated to be only 5E-07 s. Thus, we believed that there would be no decisive impact on the outcome. In our experiments, the plastic samples were placed in an alumina crucible and manually placed into the pyrolysis system. After the reactors reach the set temperature, the micro-furnace is sent to the 1st reactor and pyrolysis occurs. The reactor was maintained at 650 °C for 10 min to ensure complete pyrolysis of all samples.

Pyrolysis products were analyzed by GC/MS at a split ratio of 80:1. Helium was used as the carrier gas during the detection, and the column flow rate was 0.78 mL/min. The gas chromatograph (GC) oven was programmed to heat from 40 °C (held for 2 min) to 320 °C (held for 20 min) at a rate of 10 °C /min. Instrument parameters and detailed settings for analysis are shown in Table S2.

2.3. Chromatographic integration method

After identification of the products through mass spectra, their chromatographic peak areas were integrated for quantitative analysis. In Shimadzu GC/MS re-analysis software, there are three modes of peak integration, including automatic integration based on peak area, automatic integration based on peak height, and integration method of setting detailed parameters. The selection of integration mode and the setting of integration parameters have an important effect on the separation of different peaks, as well as the positions of the starting point and falling point of each peak, thus directly affecting the quantitative results of the peak area. Specific analysis is shown in Fig. S2 and S3. Finally, the integration parameters were set as follow: the slope limit is 10,000/min, the half-maximum width limit is 2 s, the parameter changing time is 0 min, and the minimum peak area is 1,000,000.

2.4. Selection of characteristic pyrolysis products

To select the characteristic products suitable for the present study, analytical grade samples of five types of plastic samples were detected using the standard pyrolysis condition and GC/MS analysis method. The characteristic pyrolysis products corresponding to each polymer were selected based on the comprehensive consideration of specificity and yield, with reference to the existing studies (summarized in Table S3).

2.5. Calibration of regression equations

The complexity of the matrix in environmental samples makes it difficult to select the internal standard; therefore, the external standard method was chosen in the present study. To obtain the calibration curves, standard plastic samples were weighed using a Mettler Toledo balance (New Classic MF-MS105DU) and placed into miniature crucibles for pyrolysis. In this pre-experiment, we extracted and weighed MPs from sewage sludge, and the mass range of the extracted samples was 0.09–0.53 mg. Based on this, the calibrated mass range was determined.

The calibration ranges of plastics varied depending on the pyrolysis characteristics. Taking PE as an example, the great variety of pyrolysis products results in a generally low intensity for each peak. At low masses, pyrolysis chromatographic peaks are easily deformed, and the three peaks in each peak group cannot be completely separated, which can introduce errors in the analysis process. Therefore, the lower mass limit of PE calibration was higher than that of the other plastics. For PS and PMMA, the peak intensity of the main product is maintained at a high level due to the limited kinds of pyrolysis products, and calibration can be achieved even under low quality. Correspondingly, the upper

mass limits of these two plastics should be relatively low, considering the signal detection limit of GC/MS. As for PVC, the intensity of benzene, the main product, is low due to cyclization during pyrolysis, making its upper limit higher than that of PS and PMMA.

2.6. Comparison of individual and mixed pyrolysis

Individual and mixed pyrolysis experiments were performed respectively. Their results were compared to evaluate co-pyrolysis interaction. In mixing experiments, five kinds of plastics were mixed pairwise to ten groups in a mass ratio of 1:1. The mass of each plastic sample in individual experiments was 0.40 mg to ensure a moderate intensity of the pyrolysis product peaks. In order to make the experimental results comparable, the amount of two kinds of plastic samples used in the corresponding mixed experiment was also 0.40 mg respectively. All samples were weighed by the balance and detected.

2.7. Statistical method of pyrolysis products

The pyrolysis products were classified based on two criteria. One is based on the functional groups of products, such as alkanes, alkenes, and aromatics. The other is based on the carbon number of the products, with three categories: C4 below, C5 to C12, C13 and above. The areas of all product peaks contained were summed to obtain the total for the corresponding class. The statistical results were presented as histograms. In the histogram of each plastic material, different colors are used to represent different classes, thus showing the distribution of products.

The statistical data of the same class from the individual pyrolysis of two plastic types were added correspondingly, and the data obtained were called the calculation results. While the data obtained in pairwise mixing experiments were called the experimental results. Then, the two kinds of results were compared to evaluate the influence of interaction on products distribution.

2.8. Calculation of quantitative uncertainties

The influence of interaction on characteristic products selected in Section 2.4 and subsequent quantification was studied. In pairwise mixing experiments, the peak areas of the characteristic products were obtained by integrating the chromatograms. Then through the regression equations calibrated before, we could get the calculated values of corresponding plastic mass in the mixture. Since the actual plastic mass has been weighed by the balance, the quantification uncertainties caused by the interaction could be obtained. The calculation method of uncertainties is as follows.

$$\delta = (M_{cal} - M)/M \times 100\%$$

Therein, δ is the quantification uncertainty, M_{cal} is the calculated mass using regression equations, and$M$ is the actual mass.

All the experimental runs performed repeatedly. The average and standard deviation of uncertainties were calculated and compared. The products with lower uncertainties were considered to be less affected by interaction. Thereby suitable quantitative analysis indicators for each plastic were determined.

3. Results and discussion

3.1. Characteristic pyrolysis products

Characteristics products with relatively high yields were selected according to the pyrolysis law of plastics. Pyrolysis chromatograms of the five types of plastic samples and the corresponding peaks of the selected products are shown in Fig. 1. Their specific information is listed in Table S4 and their mass spectra are shown in Fig. S4 ~ 9. These products are alternative indicators for quantitative analysis.

The chromatogram of PE has obvious regularity. In the C10–C22 stage, three peaks of diene, monoene, and alkane with the same carbon number form a group, with the peak of olefin being the highest. Pyrolysis products of high molecular mass remain in the chromatographic column, resulting in inaccurate experimental results in continuous runs. Therefore, we selected several products with relatively high yields and low molecular masses, including 2- butene, 1- pentene, 1- hexene, 1-decene, 1- undecene, 1- dodecene, 1- tridecane, 1- tetradecene, 1- pentadecene, 1- hexadecene, 1- heptadecene, and 1- octadecene.

The pyrolysis products of PP are mostly branched alkenes, among which 2,4- dimethyl − 1- heptene is the predominant product. Several substances with relatively high yields are also selected as alternatives, including 2- butene, pentane, 2- methyl − 1- pentene, and 7- methyl-undecene.

Styrene and styrene dimers are the main pyrolysis products of PS. As an alternative, bibenzyl is selected as a possible quantitative analysis indicator. Although its abundance is much lower than the two products above, it also has strong characteristics. Styrene trimer was not selected since its yield is too low.

For PVC, benzene is the most prominent peak in the pyrolysis chromatogram, and a small amount of toluene was also present. However, toluene can also be derived from the pyrolysis of PS and is not preferred. Given the limited products available, benzene was ultimately chosen, as in the M. Fischer and F. Ribeiro studies [28,31,33].

Methyl methacrylate (MMA) accounts for most of the pyrolysis products of PMMA, and the peak area proportion reaches almost 90%. At the same time, it has a strong characteristic, making it the best choice for identifying PMMA. In addition, 2- propenoic acid-methyl ester can be used as an alternative for quantitative analysis of PMMA. Although some other products, such as methyl isobutyrate, also have strong characteristics, these are not selected since their yield is too low.

To evaluate the influence of the interactions as comprehensively as possible and collect a range of quantitative analysis indicators, we selected some other peaks in PE and PP pyrolysis. These include 2-butene, 1- pentene, pentane, 1- hexene and 2- methyl − 1- pentene.

3.2. Regression equations of selected products in individual pyrolysis

Calibration experiments revealed that the products selected in the present study showed a linear relationship between the peak area and plastic mass. The regression equations and the regression coefficients obtained by calibration are listed in Table 1.

For PE, the peak area ratio of each substance was relatively low owing to the large variety of pyrolysis products. 1- Hexene had the highest abundance and the worst linearity among the alternatives, with a regression coefficient of 0.86. Monoenes with carbon numbers ranging from 10 to 18 showed good linearity, especially 1- decene, 1- undecene, 1- dodecene, 1- tridecane, and 1- octadecene, whose regression coefficients exceeded 0.99.

Among the products of PP, 2,4-dimethyl-1-heptene had the largest yield with average peak area ratio more than 20%. Although 7-methyl-1-undecene shows the best linearity, its yield is too low to detect trace PP.

Similar situations occur in the selection of the PS and PMMA indicators. As the dominant pyrolysis products of the corresponding plastics, both styrene and MMA have relatively low R^2. In contrast, bibenzyl for PS and 2-propenoic acid-methyl ester for PMMA show better performance in terms of linearity, but their low yields can lead to an increase in the quantitative detection limit.

As the main pyrolysis product of PVC, benzene performs well in both yield and linearity. It is undoubtedly the best choice for PVC quantitative analysis.

3.3. Individual pyrolysis results

The products distribution obtained by individual pyrolysis of 0.40 mg samples of the five types of plastic samples is shown in Fig. 2,

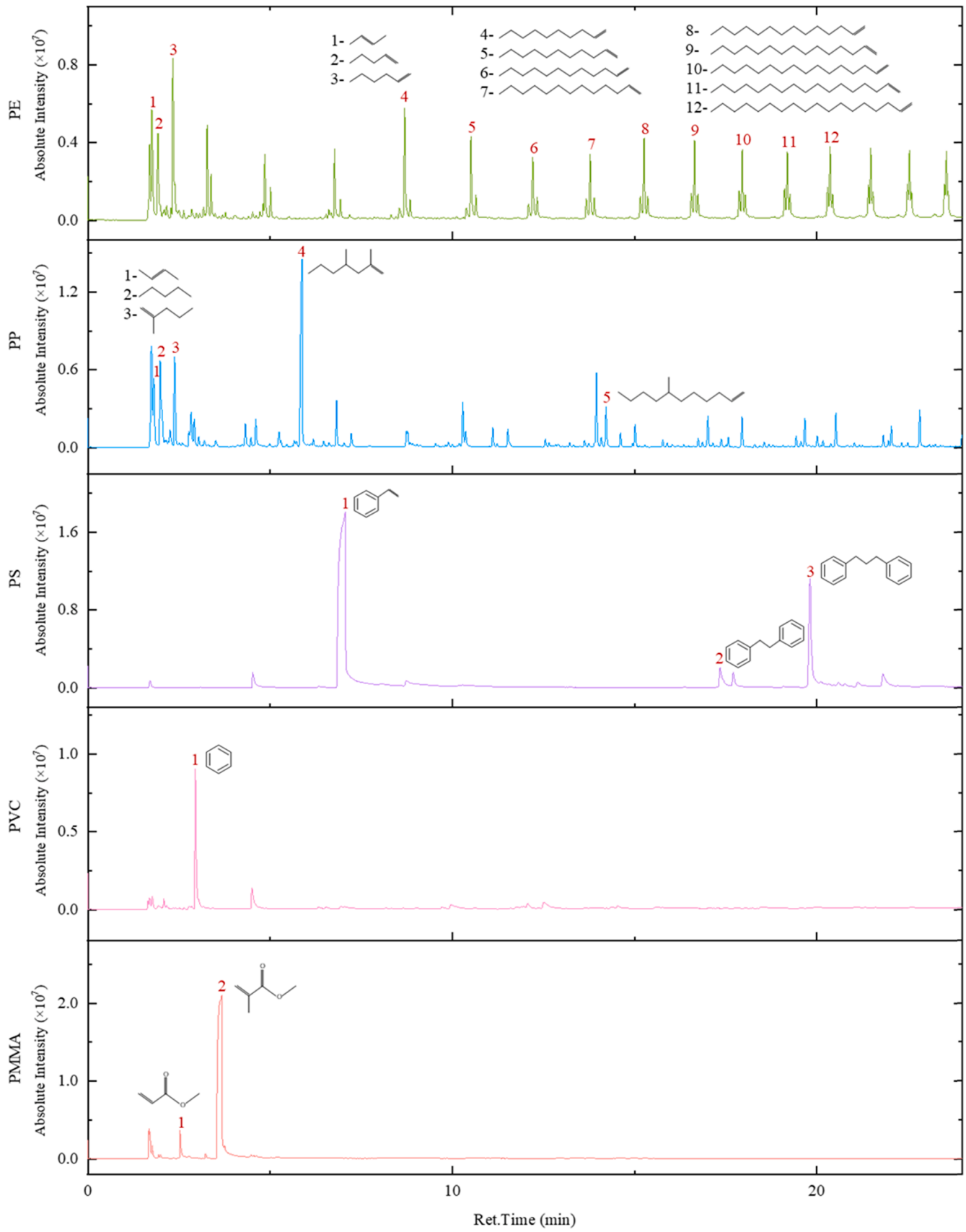

Fig. 1. Selection of characteristic chromatographic peaks of five types of plastic samples (0–25 min).

Table 1
Calibration experimental results.

Plastic	No.*	Pyrolysis Production	Peak area ratio (%)	Mass Range(mg)	N	R^2	Slope	Intercept
PE	1	2-butene	5.90 ± 1.19	0.22–0.82	9	0.977	2.86E+07	3.77E+06
	2	1-pentene	4.75 ± 0.42	0.22–0.82	9	0.967	3.21E+07	-1.24E+05
	3	1-hexene	7.32 ± 2.69	0.22–0.82	9	0.855	3.89E+07	2.34E+06
	4	1-decene	4.57 ± 0.74	0.22–0.82	9	0.995	3.14E+07	2.65E+05
	5	1-undecene	3.60 ± 0.62	0.22–0.82	9	0.996	2.71E+07	-8.72E+05
	6	1-dodecene	2.80 ± 0.38	0.22–0.82	9	0.993	2.18E+07	-1.04E+06
	7	1-tridecene	1.81 ± 0.19	0.22–0.82	9	0.992	2.19E+07	-1.17E+06
	8	1-tetradecene	2.22 ± 0.23	0.22–0.82	9	0.989	2.69E+07	-1.47E+06
	9	1-pentadecene	2.07 ± 0.23	0.22–0.82	9	0.988	2.53E+07	-1.49E+06
	10	1-hexadecene	1.79 ± 0.20	0.22–0.82	9	0.984	2.37E+07	-1.96E+06
	11	1-heptadecene	1.66 ± 0.18	0.22–0.82	9	0.988	2.20E+07	-1.83E+06
	12	1-octadecene	1.80 ± 0.18	0.22–0.82	9	0.991	2.23E+07	-1.38E+06
PP	1	2-butene	3.33 ± 0.46	0.12–0.84	12	0.956	2.48E+07	3.54E+06
	2	pentane	4.44 ± 0.91	0.12–0.84	12	0.932	5.53E+07	-2.96E+06
	3	2-methyl-1-pentene	3.56 ± 0.40	0.12–0.84	12	0.969	2.95E+07	2.84E+06
	4	2,4-dimethyl-1-heptene	22.66 ± 1.81	0.12–0.84	12	0.977	8.27E+07	1.67E+07
	5	7-methyl-1-undecene	1.77 ± 0.24	0.12–0.84	12	0.980	1.91E+07	7.84E+04
PS	1	styrene	71.29 ± 11.55	0.11–0.64	10	0.972	3.59E+08	6.06E+07
	2	bibenzyl	3.18 ± 1.06	0.23–0.64	7	0.995	4.16E+07	-5.87E+06
	3	styrene dimer	15.36 ± 2.50	0.20–0.64	9	0.967	1.36E+08	-7.59E+06
PVC	1	benzene	60.37 ± 5.89	0.18–0.83	9	0.997	4.87E+07	-3.64E+05
PMMA	1	2-propenoic acid-methyl ester	3.30 ± 1.02	0.15–0.57	9	0.998	2.22E+07	-1.35E+06
	2	methyl methacrylate	87.34 ± 3.59	0.09–0.57	10	0.989	2.95E+08	5.33E+07

Abbreviations: N = number of calibration points, R^2= coefficient of determination.
* The numbers (No.) correspond to Fig. 1.

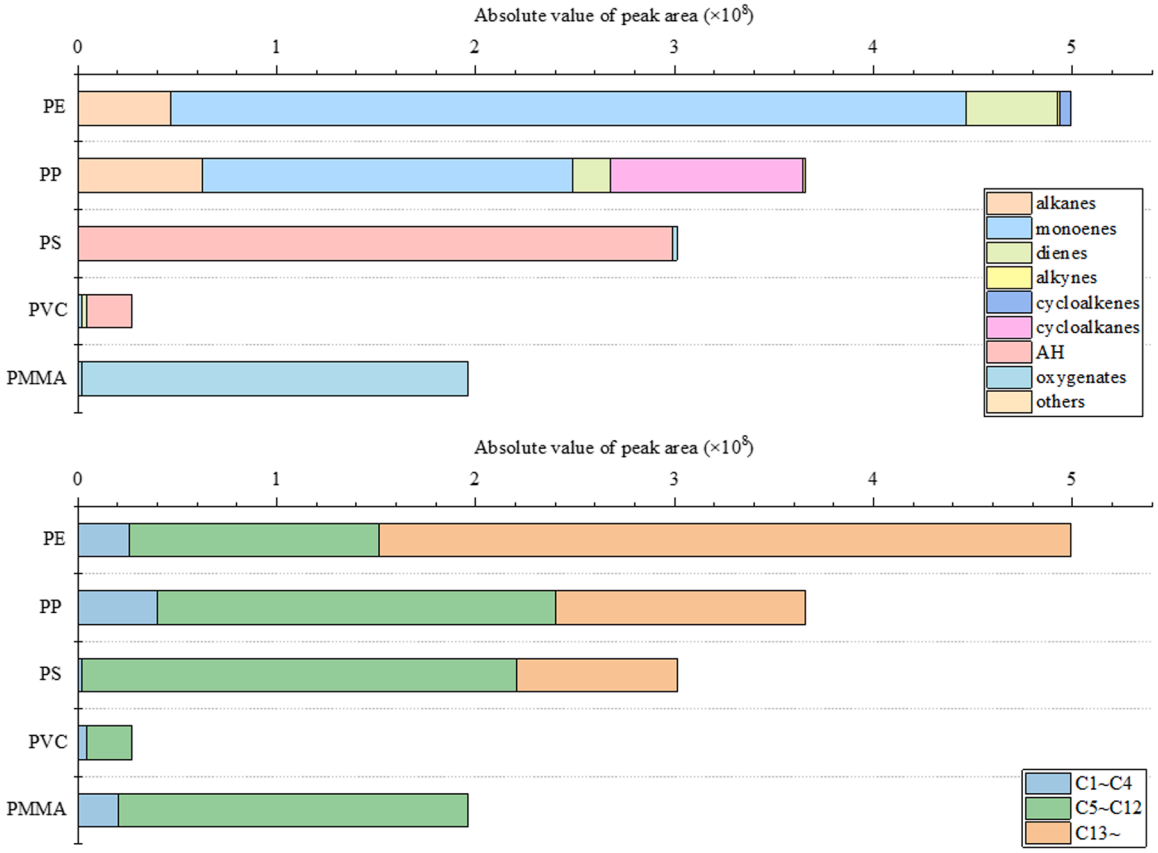

Fig. 2. Individual pyrolysis results.

where (a) and (b) are classified based on the functional group and carbon number, respectively.

The pyrolysis products of PE and PP were mainly alkanes and alkenes. As polyolefin plastics, they have similar degradation mechanism, which includes random scission and end chain scission [42,43]. In addition, the pyrolysis products of PP also contain more cycloalkanes.

For PS, the pyrolysis products are almost all AHs (aromatic hydrocarbons). During the pyrolysis process, the self-scission radical accelerates the mid-chain and end-chain β-scission by attacking the polymer chain with a phenyl radical, which leads to the formation of styrene and

end chain free radicals. The attack of free radicals on the secondary and tertiary carbons by β-scission immediately forms dimers and trimers of styrene [44].

Our experimental results show that benzene is the main pyrolysis product of PVC, which is consistent with previous studies [2]. Although HCl has also been indicated as the main pyrolysis product by several researches [2,45], it was not found in our experiment. This is because MS scanning range is *m/z* 40–650 while the relative molecular weight of HCl is 36.5. The pyrolysis of PVC can be divided into two stages. In the first stage, mainly HCl and benzene, and very few alkyl aromatic or condensed ring aromatic hydrocarbons were formed. Most double bonds in such aromatic compounds aggregate in the polymer to form a cross-linked network of cyclic compounds in the aliphatic matrix. In the second step, these cyclic compounds are aromatized by chain scission reactions to form aliphatic, olefinic, aromatic, and char [2,46].

The oxygenates account for almost all the PMMA pyrolysis products. The thermal degradation of PMMA can be divided into three or four stages. Kashiwagi et al. indicated that the pyrolysis of PMMA is first initiated by scissions of the head-to-head linkages (H-H), followed by unsaturated ends (resulting from termination by disproportionation) and random scissions within the polymer chain [47,48].

3.4. Co-pyrolysis products distribution

Fig. 3 shows the calculation results and experimental results of co-pyrolysis products distribution. Comparing the two results for each group, we found that interactions were evident in the co-pyrolysis of different polymers when using Py-GC/MS detection. In addition, PP and

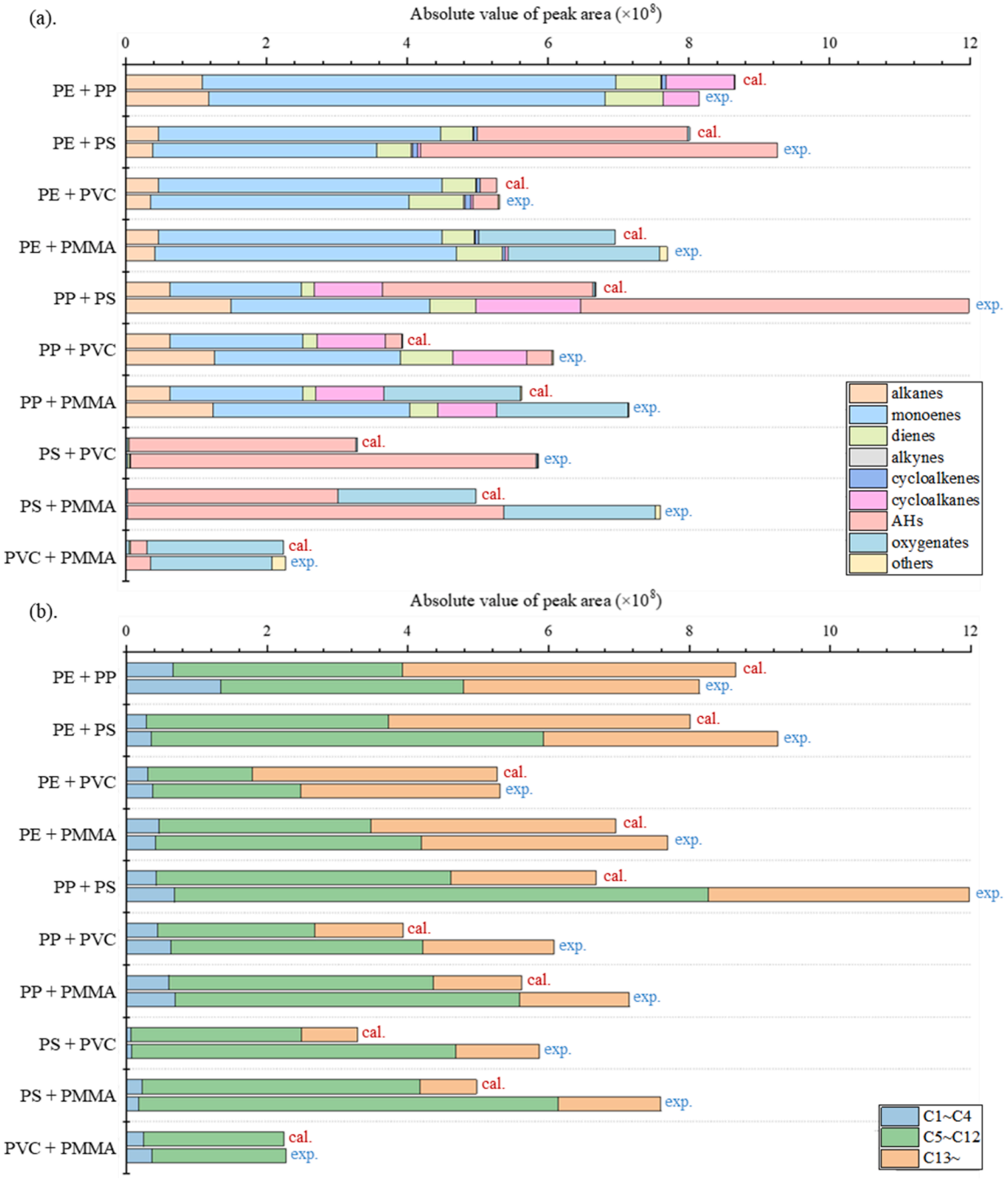

Fig. 3. Comparison between the calculated results (cal.) and the experimental results (exp.) of co-pyrolysis.

PS often exhibit strong interactions during co-pyrolysis with other plastics. Both plastics are among the most common MP components in the environment, which means ignoring the potential effects of their interactions could severely reduce the accuracy of calculations and lead to distortion in the MP pollution assessment. Specific analysis of the co-pyrolysis is as follows.

When PE was mixed with the other four plastic types, the total yields of experiments were basically consistent with the expectation. In these four groups, the mixture of PE/PS showed the most significant difference between the calculation and experimental results, mainly reflected in monoenes and AHs. Meanwhile, the specific analysis showed that both the species and yield of the AHs in co-pyrolysis increased, showing a strong promotion of interaction. R. K. Singh et al. pointed out that the reaction is followed by β-scission to produce styrene and chain end free radical during the degradation of PS. Early initiation of end chain and β-scission causes the degradation of PE at a lower temperature [37]. Wu et al. indicated through FTIR analysis that new unsaturated hydrocarbon groups are produced, and alkyne groups disappear during co-pyrolysis

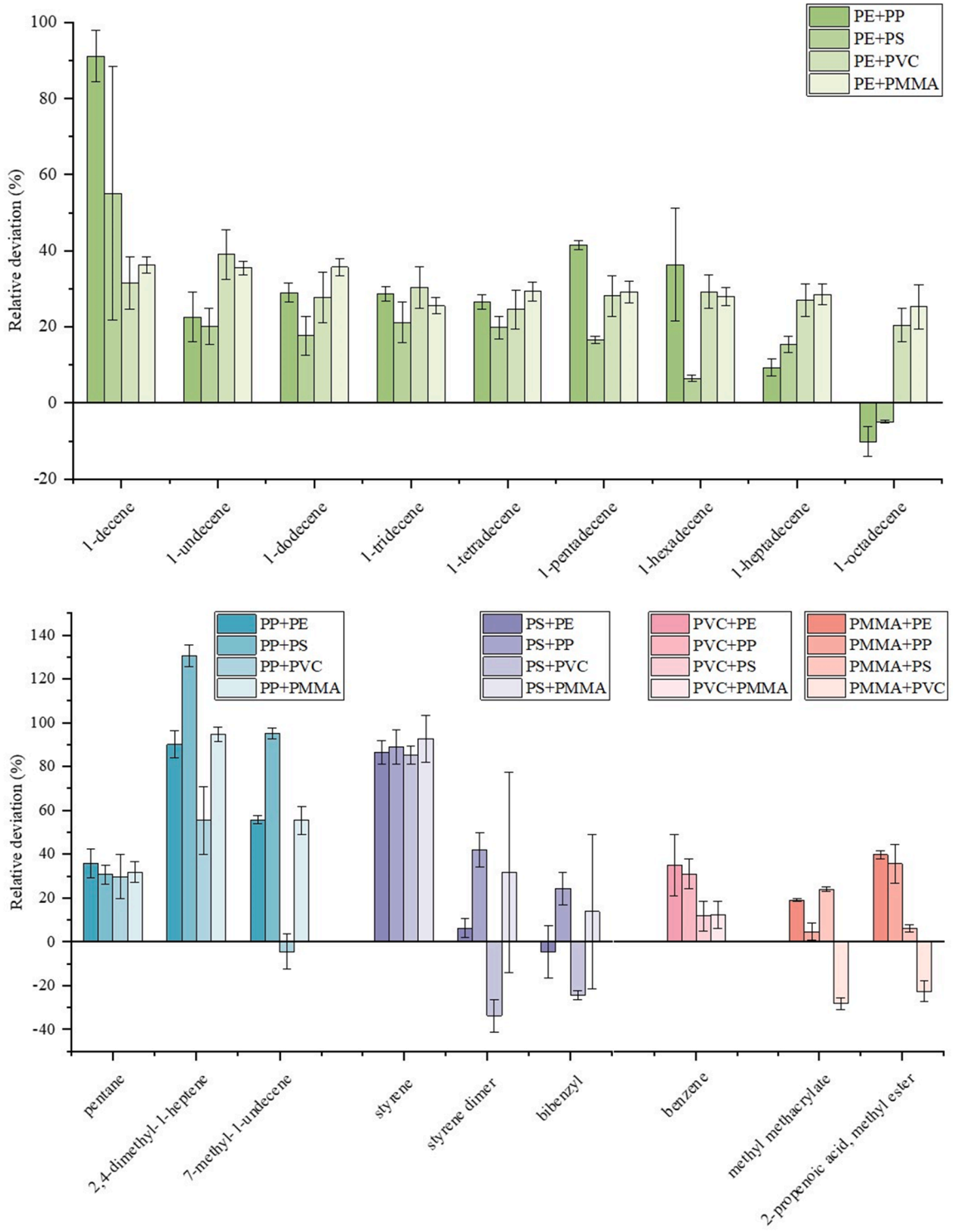

Fig. 4. Representative uncertainty data in mixture experiments (* the peak area of pentane is obtained by calculation rather than direct integration).

[41], but this is inconsistent with our experimental results, where alkynes were also found in the products of co-pyrolysis.

The co-pyrolysis of PE/PP obviously reduced the yield of cycloalkanes and showed a significant trend of lightweights according to the product distribution based on carbon number. It has been found in the previous research that the co-pyrolysis reaction rate curve did not show the separated PE and PP peaks but a single peak with a synergistic effect [37]. The authors speculated the existence of PE limited the degradation of PP at lower temperatures and delayed the degradation process.

For PP, its blends with PS/PVC/PMMA all received the experimental results that were quite different from calculations.

In the co-pyrolysis experiments of PP/PS, the yields of all products were much higher than expected. Through specific analysis, we found a significantly greater variety of products in the mixed pyrolysis. More than ten kinds of new AHs, such as 2- acryl-benzene, 3-butenyl-benzene, and 3-methyl-3-butenyl-benzene, were detected, presumably the result of the secondary reaction of the pyrolysis products in a high-temperature environment. This is basically consistent with previous research conclusions. In 2017, Sophonrat et al. found that PP/PS co-pyrolysis has interaction [49].

Strong interactions were also exhibited in the co-pyrolysis of PS/PVC and PS/PMMA, with a significant increase in yields.

For PS/PVC mixture, more than ten new product species emerged, such as 1,1'-(1,3-propanediyl) bis-benzene. Several studies have indicated that the dehydrochlorination of PVC is inhibited during the co-pyrolysis of PS/PVC [50,51], but this conclusion could not be validated because HCl could not be detected in this experiment.

In the co-pyrolysis experiment of PS/PMMA, the AHs content was much higher than expected, which means that the interaction can promote the pyrolysis of PS. On the other hand, there is no obvious change in the yield of oxygenates as the pyrolysis product of PMMA and the specific types are completely consistent with those of single-component pyrolysis, indicating that PMMA is less affected.

3.5. Quantification uncertainties of indicators in co-pyrolysis

The plastic mass in the mixture was calculated using the regression equations described above. For each indicator, the deviations between the calculated results and the mass values weighed by the balance are summarized in Fig. 4.

A total of 18 groups of histograms are shown. 1-decene, 1- undecene, 1- dodecene, 1- tridecane, 1- tetradecene, 1- pentadecene, 1- hexadecene, 1- heptadecane, and 1- octadecene correspond to PE. Pentane, 2,4- dimethyl − 1- heptene, and 7- methyl − 1- undecene correspond to PP. Styrene, styrene dimer, and bibenzyl correspond to PS. Benzene corresponds to PVC. Both MMA and 2-propenoic acid-methyl ester correspond to PMMA.

Among the nine PE pyrolysis products evaluated, 1-decene was the least satisfactory, with the calculated result being nearly 90% higher than the actual value by when PE and PP are equally mixed. Similarly, 1-pentadecene and 1- hexadecene were not considered because of the increased uncertainty in the PE/PP mixing experiments. Several monoenes with carbon numbers of 11–14 were present at the same level, with uncertainties of 20–40%. The final comprehensive comparison shows that 1- octadecene is the most suitable quantitative indicator for PE. Under the four mixing modes, PE/PP, PE/PS, PE/PVC, and PE/PMMA, the average uncertainty values were − 10.12%, − 4.99%, 20.44%, and 25.25%, respectively. Given that the PE, PP, and PS levels in the environment are much higher than those of other plastics, we are more concerned about the effects caused by the mixing of these three plastics, so the performance of 1- octadecene is considered acceptable.

2,4- dimethyl − 1- heptene, as the main product of PP pyrolysis, was selected as a quantitative indicator in previous MP studies. However, our experimental results show that this calculation method may produce considerable uncertainties, reaching 130% when PP/PS is mixed. Simultaneously, in the PP/PE, PP/PVC, and PP/PMMA mixing experiments, the uncertainty reached 90.13%, 55.39%, and 94.85%, respectively. The performance of 7- methyl − 1- undecane is better than 2,4-dimethyl − 1- heptene, especially in the PP/PVC mixture, when the uncertainty was controlled within 10%. However, with more than 95% uncertainty in the PP/PS mixtures, 7- methyl − 1- undecane was not selected as a quantitative indicator. Pentane was ultimately selected as a quantitative indicator of PP. In order to eliminate the influence of overlapping with the peak of 1- pentene due to the similar retention time, as shown in Fig. S10, specific calculation method was developed as: (i) using 1- octadecene to estimate the quality of PE, the peak area of 1- pentene generated from PE pyrolysis was calculated from its regression equation; (ii) The calculated result was deduced from the integral area of overlapping peaks in the mixed pyrolysis to obtain the peak area of pentane generated from PP pyrolysis. Finally, the mass of PP was calculated using the pentane regression equation.

In the mixing experiment of PS with the other four plastics, the yield of styrene significantly increased due to the interaction, resulting in a calculation uncertainty of more than 85%. The styrene dimer and bibenzyl were much less affected by the co-pyrolysis. In the PS/PE mixture, the calculation uncertainties of the two indicators were within ± 10%. Comparatively, the quantitative accuracy of bibenzyl was better. The average uncertainties in the four mixed modes were − 4.56%, 24.25%, − 24.55%, and 13.82%, respectively.

For PVC, benzene is the only quantitative indicator choice due to limited pyrolysis products. From the specific experimental results, PE and PP have a greater impact on the PVC quantification, with uncertainties exceeding 30%. In the mixture with PS and PMMA, the uncertainties were 11.70% and 12.41%, respectively, which were satisfactory. Overall, benzene showed good reliability in the mixing experiments.

For PMMA, we compared the accuracy of MMA and 2-propenoic acid-methyl ester in quantitative calculations. The experimental results showed that although the calculation uncertainty of MMA was higher in the co-pyrolysis with PS and PVC, its reliability was much better than that of 2-propenoic acid-methyl ester in the mixing experiment with PE and PP. Overall, MMA is less affected by interaction and is undoubtedly the best choice for quantitative analysis, considering its much higher yield.

Finally, 1- octadecene, pentane, and bibenzyl were selected as new indicators for PE, PP, and PS, respectively. Fig. 5 shows the quantitative uncertainty ranges of the indicators selected in the present and previous researches [28,29,31–33,35,52]. Our method significantly improves quantitative accuracy.

4. Conclusion

The present study focused on improving the accuracy of quantitative detection of five common MPs components based on Py-GC/MS. It was found that some commonly used quantitative indicators were subject to high uncertainty due to co-pyrolysis interaction. They are thus not suitable for the detection of mixed MPs samples. Through comparison, 1- octadecene, pentane, and bibenzyl were selected as new indicators for PE, PP, and PS, respectively. While some other existing indicators, including benzene and MMA, showed good accuracy in mixing experiments. Therefore, we didn't propose new indicators but maintained the original selections for PVC and PMMA.

With the interaction fully considered, we improved the detection method and obtained significant results. The upper limit of quantification uncertainty of PE was reduced from 91% to 25%, that of PP from 130–32%, and that of PS from 93–24%. This research has far-reaching significance in the application of Py-GC/MS in the quantification of mixed MPs.

CRediT authorship contribution statement

Fangfang Lou: Conceptualization, Investigation, Project

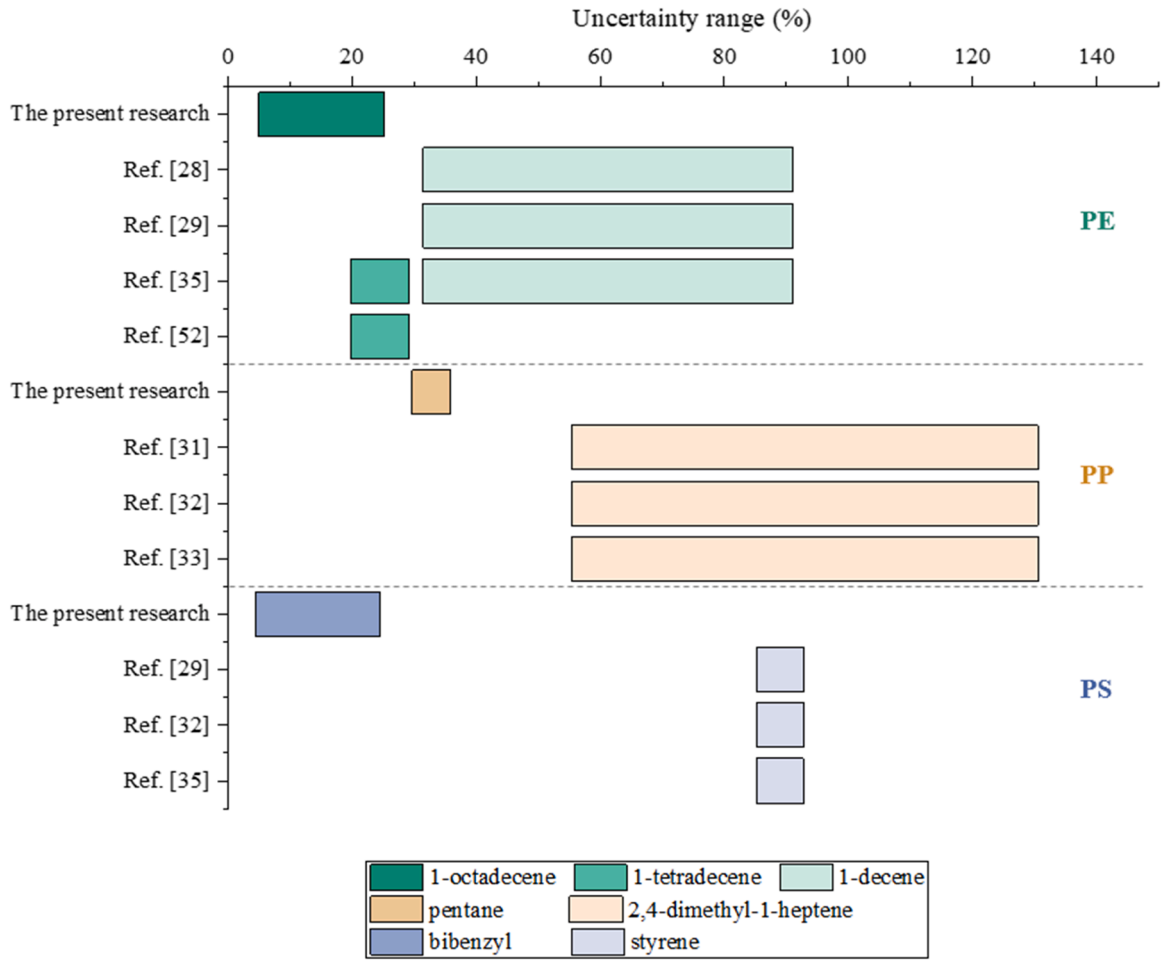

Fig. 5. Uncertainty range of the indicators.

administration, Roles/Writing – original draft. **Jun Wang:** Formal analysis. **Chen Sun:** Methodology. **Jiaxing Song:** Validation. **Wanli Wang:** Data curation. **Yuhan Pan:** Software. **Qunxing Huang:** Funding acquisition, Writing – review & editing. **Jianhua Yan:** Supervision.

Declaration of Competing Interest

The authors declare that they have no known competing financial interests or personal relationships that could have appeared to influence the work reported in this paper.

Acknowledgments

The authors would like to gratefully acknowledge the National Natural Science Foundation of China (52076190), Key Research and Development Program of Zhejiang Province (2022C03082), and Zhejiang University Ecological Civilization Plan.

Appendix A. Supporting information

Supplementary data associated with this article can be found in the online version at doi:10.1016/j.jece.2022.108012.

References

[1] R.C. Thompson, Y. Olsen, R.P. Mitchell, A. Davis, S.J. Rowland, A.W.G. John, D. Mcgonigle, A.E. Russell, Lost at sea: where is all the plastic? Science 304 (5672) (2004) https://doi.org/10.1126/science.1094559.

[2] A. Bhargava, P. Van Hees, B. Andersson, Pyrolysis modeling of PVC and PMMA using a distributed reactivity model, Polym. Degrad. Stab. 129 (2016) 199–211, https://doi.org/10.1016/j.polymdegradstab.2016.04.016.

[3] M. Cole, P. Lindeque, E. Fileman, C. Halsband, R. Goodhead, J. Moger, T. S. Galloway, Microplastic ingestion by zooplankton, Environ. Sci. Technol. 47 (12) (2013) 6646–6655, https://doi.org/10.1021/es400663f.

[4] L.I. Devriese, M.D. Van Der Meulen, T. Maes, K. Bekaert, I. Paul-Pont, L. Frere, J. Robbens, A.D. Vethaak, Microplastic contamination in brown shrimp (Crangon crangon, Linnaeus 1758) from coastal waters of the Southern North Sea and Channel area, Mar. Pollut. Bull. 98 (1–2) (2015) 179–187, https://doi.org/10.1016/j.marpolbul.2015.06.051.

[5] C.O. Egbeocha, S. Malek, C.U. Emenike, P. Milow, Feasting on microplastics: ingestion by and effects on marine organisms, Aquat. Biol. 27 (2018) 93–106, https://doi.org/10.3354/ab00701.

[6] S. Savoca, G. Capillo, M. Mancuso, T. Bottari, R. Crupi, C. Branca, V. Romano, C. Faggio, G. D'angelo, N. Spano, Microplastics occurrence in the Tyrrhenian waters and in the gastrointestinal tract of two congener species of seabreams, Environ. Toxicol. Pharmacol. 67 (2019) 35–41, https://doi.org/10.1016/j.etap.2019.01.011.

[7] P. Pannetier, B. Morin, F. Le Bihanic, L. Dubreil, C. Clerandeau, F. Chouvellon, K. Van Arkel, M. Danion, J. Cachot, Environmental samples of microplastics induce significant toxic effects in fish larvae, Environ. Int. 134 (2020), 105047, https://doi.org/10.1016/j.envint.2019.105047.

[8] J. Oehlmann, U. Schulte-Oehlmann, W. Kloas, O. Jagnytsch, C.R. Tyler, A critical analysis of the biological impacts of plasticizers on wildlife, Philos. Trans. R. Soc. B Biol. Sci. 364 (1526) (2009) 2047–2062.

[9] E. Chris, Talsness, J. Anderson, M. Andrade, N. Sergio, Kuriyama, Components of plastic: experimental studies in animals and relevance for human health, Philos. Trans. R. Soc. B Biol. Sci. 364 (1526) (2009) 2079–2096.

[10] L.A. Holmes, A. Turner, R.C. Thompson, Interactions between trace metals and plastic production pellets under estuarine conditions, Mar. Chem. 167 (2014) 25–32, https://doi.org/10.1016/j.marchem.2014.06.001.

[11] A. Turner, L.A. Holmes, Adsorption of trace metals by microplastic pellets in fresh water, Environ. Chem. 12 (5) (2015) 600–610, https://doi.org/10.1071/En14143.

[12] A. Bakir, S.J. Rowland, R.C. Thompson, Competitive sorption of persistent organic pollutants onto microplastics in the marine environment, Mar. Pollut. Bull. 64 (12) (2012) 2782–2789, https://doi.org/10.1016/j.marpolbul.2012.09.010.

[13] A. Bakir, S.J. Rowland, R.C. Thompson, Enhanced desorption of persistent organic pollutants from microplastics under simulated physiological conditions, Environ. Pollut. 185 (2014) 16–23, https://doi.org/10.1016/j.envpol.2013.10.007.
[14] J.P.G.L. Frias, P. Sobral, A.M. Ferreira, Organic pollutants in microplastics from two beaches of the Portuguese coast, Mar. Pollut. Bull. 60 (11) (2010) 1988–1992, https://doi.org/10.1016/j.marpolbul.2010.07.030.
[15] S.L. Wright, R.C. Thompson, T.S. Galloway, The physical impacts of microplastics on marine organisms: a review, Environ. Pollut. 178 (2013) 483–492, https://doi.org/10.1016/j.envpol.2013.02.031.
[16] G. Liebezeit, F. Dubaish, Microplastics in beaches of the East Frisian Islands Spiekeroog and Kachelotplate, Bull. Environ. Contam. Toxicol. 89 (1) (2012) 213–217, https://doi.org/10.1007/s00128-012-0642-7.
[17] C.M. Free, O.P. Jensen, S.A. Mason, M. Eriksen, N.J. Williamson, B. Boldgiv, High-levels of microplastic pollution in a large, remote, mountain lake, Mar. Pollut. Bull. 85 (1) (2014) 156–163, https://doi.org/10.1016/j.marpolbul.2014.06.001.
[18] R. Lenz, K. Enders, C.A. Stedmon, D.M.A. Mackenzie, T.G. Nielsen, A critical assessment of visual identification of marine microplastic using Raman spectroscopy for analysis improvement, Mar. Pollut. Bull. 100 (1) (2015) 82–91, https://doi.org/10.1016/j.marpolbul.2015.09.026.
[19] J.H. Dekiff, D. Remy, J. Klasmeier, E. Fries, Occurrence and spatial distribution of microplastics in sediments from Norderney, Environ. Pollut. 186 (2014) 248–256, https://doi.org/10.1016/j.envpol.2013.11.019.
[20] A. Kappler, M. Fischer, B.M. Scholz-Bottcher, S. Oberbeckmann, M. Labrenz, D. Fischer, K.J. Eichhorn, B. Voit, Comparison of mu-ATR-FTIR spectroscopy and py-GCMS as identification tools for microplastic particles and fibers isolated from river sediments, Anal. Bioanal. Chem. 410 (21) (2018) 5313–5327, https://doi.org/10.1007/s00216-018-1185-5.
[21] Z. Zhang, Y. Su, J. Zhu, J. Shi, H. Huang, B. Xie, Distribution and removal characteristics of microplastics in different processes of the leachate treatment system, Waste Manag. 120 (2021) 240–247, https://doi.org/10.1016/j.wasman.2020.11.025.
[22] B. Chai, Q. Wei, Y. She, G. Lu, Z. Dang, H. Yin, Soil microplastic pollution in an e-waste dismantling zone of China, Waste Manag. 118 (2020) 291–301, https://doi.org/10.1016/j.wasman.2020.08.048.
[23] D. Schymanski, C. Goldbeck, H.-U. Humpf, P. Fürst, Analysis of microplastics in water by micro-Raman spectroscopy: release of plastic particles from different packaging into mineral water, Water Res. 129 (2018) 154–162, https://doi.org/10.1016/j.watres.2017.11.011.
[24] S. Fortin, B. Song, C. Burbage, Quantifying and identifying microplastics in the effluent of advanced wastewater treatment systems using Raman microspectroscopy, Mar. Pollut. Bull. 149 (2019), 110579, https://doi.org/10.1016/j.marpolbul.2019.110579.
[25] Y. Zhang, Y. Peng, C. Peng, P. Wang, Y. Lu, X. He, L. Wang, Comparison of detection methods of microplastics in landfill mineralized refuse and selection of degradation degree indexes, Environ. Sci. Technol. 55 (20) (2021) 13802–13811, https://doi.org/10.1021/acs.est.1c02772.
[26] H.K. Imhof, C. Laforsch, A.C. Wiesheu, J. Schmid, P.M. Anger, R. Niessner, N. P. Ivleva, Pigments and plastic in limnetic ecosystems: a qualitative and quantitative study on microparticles of different size classes, Water Res. 98 (2016) 64–74, https://doi.org/10.1016/j.watres.2016.03.015.
[27] T. Mani, S. Primpke, C. Lorenz, G. Gerdts, P. Burkhardt-Holm, Microplastic pollution in Benthic Midstream Sediments of the Rhine River, Environ. Sci. Technol. 53 (10) (2019) 6053–6062, https://doi.org/10.1021/acs.est.9b01363.
[28] F. Ribeiro, E.D. Okoffo, J.W. O'brien, S. Fraissinet-Tachet, S. O'brien, M. Gallen, S. Samanipour, S. Kaserzon, J.F. Mueller, T. Galloway, K.V. Thomas, Quantitative analysis of selected plastics in high-commercial-value australian seafood by pyrolysis gas chromatography mass spectrometry, Environ. Sci. Technol. 54 (15) (2020) 9408–9417, https://doi.org/10.1021/acs.est.0c02337.
[29] Y. Liu, R. Li, J. Yu, F. Ni, Y. Sheng, A. Scircle, J.V. Cizdziel, Y. Zhou, Separation and identification of microplastics in marine organisms by TGA-FTIR-GC/MS: a case study of mussels from coastal China, Environ. Pollut. 272 (2021), 115946, https://doi.org/10.1016/j.envpol.2020.115946.
[30] C. Goedecke, D. Dittmann, P. Eisentraut, Y. Wiesner, B. Schartel, P. Klack, U. Braun, Evaluation of thermoanalytical methods equipped with evolved gas analysis for the detection of microplastic in environmental samples, J. Anal. Appl. Pyrolysis 152 (2020), 104961, https://doi.org/10.1016/j.jaap.2020.104961.
[31] M. Fischer, B.M. Scholz-Bottcher, Simultaneous trace identification and quantification of common types of microplastics in environmental samples by pyrolysis-gas chromatography-mass spectrometry, Environ. Sci. Technol. 51 (9) (2017) 5052–5060, https://doi.org/10.1021/acs.est.6b06362.
[32] Z. Steinmetz, A. Kintzi, K. Munoz, G.E. Schaumann, A simple method for the selective quantification of polyethylene, polypropylene, and polystyrene plastic debris in soil by pyrolysis-gas chromatography/mass spectrometry, J. Anal. Appl. Pyrolysis 147 (2020), 104803, https://doi.org/10.1016/j.jaap.2020.104803.
[33] M. Fischer, B.M. Scholz-Bottcher, Microplastics analysis in environmental samples - recent pyrolysis-gas chromatography-mass spectrometry method improvements to increase the reliability of mass-related data, Anal. Methods 11 (18) (2019) 2489–2497, https://doi.org/10.1039/c9ay00600a.
[34] E. Hendrickson, E.C. Minor, K. Schreiner, Microplastic abundance and composition in western lake superior as determined via microscopy, Pyr-GC/MS, and FTIR, Environ. Sci. Technol. 52 (4) (2018) 1787–1796, https://doi.org/10.1021/acs.est.7b05829.
[35] I.V. Kirstein, F. Hensel, A. Gomiero, L. Iordachescu, A. Vianello, H.B. Wittgren, J. Vollertsen, Drinking plastics? - quantification and qualification of microplastics in drinking water distribution systems by mu FTIR and Py-GCMS, Water Res. 188 (2021), 116519, https://doi.org/10.1016/j.watres.2020.116519.
[36] L. Hermabessiere, C. Himber, B. Boricaud, M. Kazour, R. Amara, A.L. Cassone, M. Laurentie, I. Paul-Pont, P. Soudant, A. Dehaut, G. Duflos, Optimization, performance, and application of a pyrolysis-GC/MS method for the identification of microplastics, Anal. Bioanal. Chem. 410 (25) (2018) 6663–6676, https://doi.org/10.1007/s00216-018-1279-0.
[37] R.K. Singh, B. Ruj, A.K. Sadhukhan, P. Gupta, A TG-FTIR investigation on the co-pyrolysis of the waste HDPE, PP, PS and PET under high heating conditions, J. Energy Inst. 93 (3) (2020) 1020–1035, https://doi.org/10.1016/j.joei.2019.09.003.
[38] M.N. Siddiqui, H.H. Redhwi, Pyrolysis of mixed plastics for the recovery of useful products, Fuel Process. Technol. 90 (4) (2009) 545–552, https://doi.org/10.1016/j.fuproc.2009.01.003.
[39] P. Costa, F. Pinto, A.M. Ramos, I. Gulyurtlu, I. Cabrita, M.S. Bernardo, Study of the pyrolysis kinetics of a mixture of polyethylene, polypropylene, and polystyrene, Energy Fuels 24 (12) (2010) 6239–6247, https://doi.org/10.1021/ef101010n.
[40] P.T. Williams, E.A. Williams, Interaction of plastics in mixed-plastics pyrolysis, Energy Fuels 13 (1) (1999) 188–196, https://doi.org/10.1021/ef980163x.
[41] J.L. Wu, T.J. Chen, X.T. Luo, D.Z. Han, Z.Q. Wang, J.H. Wu, TG/FTIR analysis on co-pyrolysis behavior of PE, PVC and PS, Waste Manag. 34 (3) (2014) 676–682, https://doi.org/10.1016/j.wasman.2013.12.005.
[42] K. Murata, Y. Hirano, Y. Sakata, M.A. Uddin, Basic study on a continuous flow reactor for thermal degradation of polymers, J. Anal. Appl. Pyrolysis 65 (1) (2002) 71–90, https://doi.org/10.1016/S0165-2370(01)00181-4.
[43] K. Murata, K. Sato, Y. Sakata, Effect of pressure on thermal degradation of polyethylene, J. Anal. Appl. Pyrolysis 71 (2) (2004) 569–589, https://doi.org/10.1016/j.jaap.2003.08.010.
[44] A. Guyot, Recent developments in the thermal-degradation of polystyrene - a review, Polym. Degrad. Stab. 15 (3) (1986) 219–235, https://doi.org/10.1016/0141-3910(86)90052-2.
[45] Z. Ahmad, F. Al-Sagheer, N.A. Al-Awadi, Pyro-GC/MS and thermal degradation studies in polystyrene-poly(vinyl chloride) blends, J. Anal. Appl. Pyrolysis 87 (1) (2010) 99–107, https://doi.org/10.1016/j.jaap.2009.10.010.
[46] I.C. Mcneill, L. Memetea, W.J. Cole, A study of the products of Pvc thermal-degradation, Polym. Degrad. Stab. 49 (1) (1995) 181–191, https://doi.org/10.1016/0141-3910(95)00064-S.
[47] T. Kashiwagi, A. Inaba, J.E. Brown, K. Hatada, T. Kitayama, E. Masuda, Effects of weak linkages on the thermal and oxidative-degradation of poly(Methyl Methacrylates), Macromolecules 19 (8) (1986) 2160–2168, https://doi.org/10.1021/ma00162a010.
[48] M. Ferriol, A. Gentilhomme, M. Cochez, N. Oget, J.L. Mieloszynski, Thermal degradation of poly(methyl methacrylate) (PMMA): modelling of DTG and TG curves, Polym. Degrad. Stab. 79 (2) (2003) 271–281, https://doi.org/10.1016/S0141-3910(02)00291-4.
[49] N. Sophonrat, L. Sandström, A.-C. Johansson, W. Yang, Co-pyrolysis of mixed plastics and cellulose: an interaction study by Py-GC×GC/MS, Energy Fuels 31 (10) (2017) 11078–11090, https://doi.org/10.1021/acs.energyfuels.7b01887.
[50] I.C. Mcneill, D. Neil, A. Guyot, M. Bert, A. Michel, Thermal degradation of graft copolymers of Pvc prepared by mastication with styrene and methyl methacrylate, and of further Pvc mixtures and vinyl chloride copolymers, Eur. Polym. J. 7 (5) (1971) 453–469, https://doi.org/10.1016/0014-3057(71)90079-6.
[51] B. Dodson, I.C. Mcneill, Degradation of polymer mixtures.6. Blends of polyvinyl-chloride with polystyrene, J. Polym. Sci. Part a Polym. Chem. 14 (2) (1976) 353–364, https://doi.org/10.1002/pol.1976.170140208.
[52] A. Gomiero, K.B. Oysaed, L. Palmas, G. Skogerbo, Application of GCMS-pyrolysis to estimate the levels of microplastics in a drinking water supply system, J. Hazard. Mater. 416 (2021), 125708, https://doi.org/10.1016/j.jhazmat.2021.125708.